

## Plastic Deformation of Nanometer-Scale Gold Connective Necks

N. Agrait, G. Rubio, and S. Vieira

*Instituto Universitario de Ciencia de Materiales "Nicolás Cabrera" Laboratorio de Bajas Temperaturas, C-III, Universidad Autónoma de Madrid, 28049 Madrid, Spain*

(Received 29 July 1994)

A combined scanning force and tunneling microscope is used to study the plastic deformation of a connective neck of nanometer dimensions formed by cohesive bonding between metal tip and substrate after contact. The applied force and conductance of the neck are measured simultaneously during the deformation process, which proceeds in alternating elastic and yielding stages. From these data the Young's modulus and the yield stress of the neck are estimated. This is the first experimental quantitative measurement of plastic deformation in a structure of nanometer size.

PACS numbers: 61.16.Ch, 62.20.Fe, 73.40.Cg

Materials science has found new and exciting tools following the development of the scanning tunneling microscope (STM), after which other instruments based on similar principles have been developed [1]. The possibility of studying the processes that occur at the atomic level when two materials are brought into contact is very promising for understanding problems of enormous basic and technological interest such as contact formation, adhesion, friction, wear, fracture dynamics, materials hardness, surface deformations, and many others.

Macroscopic contact between two bodies is the result of contact between microscopic asperities, and consequently the nanomechanical properties of these asperities will be responsible for the macroscopic behavior. Recently several groups have reported molecular dynamics calculations [2–4] which provide deep insight on several aspects of the formation, plastic deformation, and fracture of the connective neck formed when a clean metal asperity interacts with a clean metal surface.

In this Letter, we present a detailed experimental study of the nanomechanical behavior of the connective necks formed between a tip and a substrate of the same metal (Au) by cohesive bonding after contact. The radius of these necks ranges from 1 to 8 nm. This experimental approach is quite different from that of other nanomechanical studies [5,6] in which a hard tip of about 100 nm radius indents a softer material substrate. In previous work we studied the plastic deformation of Pb connective necks [7] using an STM. The stepwise variation of the conductance as the tip was moved perpendicularly to the substrate was attributed to the alternation of elastic and yielding stages during the deformation process. Now we have added force measuring capability to make possible a complete characterization of metal connective necks from a nanomechanical point of view. To our knowledge this is the first quantitative experimental report to follow the plastic deformation process with such minute detail.

The experimental setup is shown in the inset of Fig. 1. The force exerted by the Au tip on the Au substrate is obtained by measuring the deflection of a stiff

phosphorous bronze cantilever (elastic constant 705 N/m) on which the substrate is mounted, with an auxiliary tunneling tip. This auxiliary tunneling tip works in the constant current mode, that is, at constant tunneling gap distance, and consequently forces exerted by this tip on the cantilever are constant and need not be taken into account [8]. In addition to the tunneling voltage applied between the auxiliary STM tip and the cantilever, we apply a voltage difference of 10 mV [9] between the Au tip and Au substrate in order to measure the neck conductance. This is the same setup we used in a previous work [10], but with improved resolution. The experiment is conducted in vacuum at liquid helium temperature (4.2 K). Under this condition thermal drift and creep effects in the piezoelectric transducers [11] are negligible, and capillary forces are completely avoided, resulting in a very good reproducibility of the measurements.

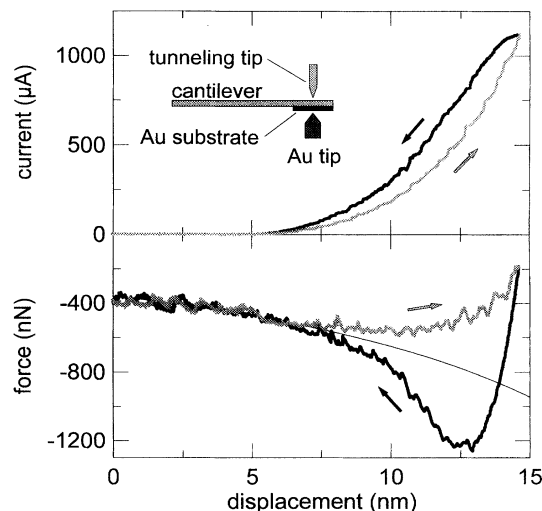


FIG. 1. 15 nm amplitude load-cycle. Force and current vs displacement. Thin line is the extrapolation of the long-range attractive force before contact, which is used as the line of zero mechanical force. Inset: Experimental setup.

The tip-substrate contact area is obtained from the conductance of the neck, which for necks of radius much smaller than the mean free path of the electrons (larger than 100 nm for gold at low temperatures) depends only on the neck radius and not on the resistivity of the material [12,13]. The current is a good probe of changes in the neck geometry because all the mechanical stresses are concentrated in the narrowest part of the neck [2], and consequently, it is there where changes will be more pronounced.

After selecting a spot on the substrate, repeated load-cycles are performed by moving the tip toward the substrate at a constant speed and reversing the motion after a given amplitude has been reached. During the cycle, the deflection of the cantilever (proportional to the force) and the current between Au tip and substrate (proportional to the conductance) are simultaneously acquired. When tip and substrate contact, they are bonded by cohesive forces, and on retraction a connective neck is formed. As the tip is further retracted this neck deforms plastically and finally breaks. After breaking the neck, we can image the contact area scanning the Au substrate with the Au tip: a protrusion, whose size depends on the maximum load, is observed at the spot where the neck was formed (see Fig. 2). We may assume that a similar protrusion has been formed on the tip. The fact that a protrusion is formed after separation indicates that any adsorbates on the contacting surfaces have been displaced from the junction until a clean metal-metal cohesive bonding has formed [14]. Repeating the load-cycle at the same spot results in an alternate formation and breaking of the neck. In Fig. 1, we show one of such repeated load-cycles. On the horizontal axis we have plotted the relative displacement between tip and substrate by subtracting at each point the motion of the can-

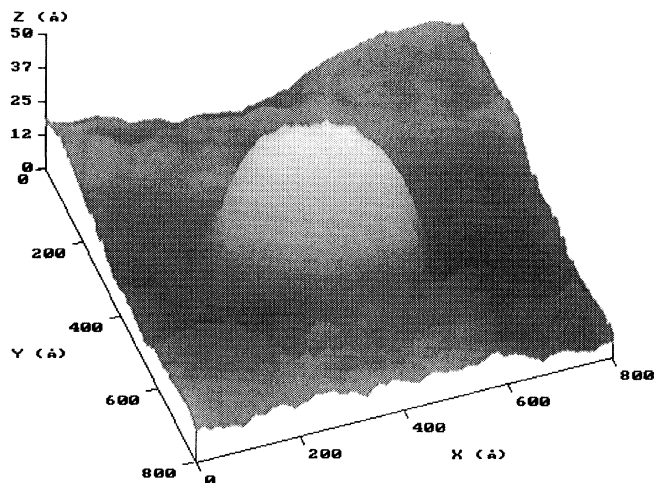


FIG. 2. Protrusion on the substrate after breaking of the connective neck. A series of load-cycles of an amplitude, similar to that of the load-cycle in Fig. 1, were performed on this spot. Bias voltage was 100 mV (tip negative), and the current was 1 nA.

tilever. In this figure, forces are considered negative when the cantilever bends downwards, i.e., toward the Au tip, which corresponds to attractive or tensile forces, and positive when the cantilever bends upwards, i.e., away from the Au tip, which corresponds to repulsive or compressive forces. Mechanical contact is signaled by the jump-to-contact phenomenon, which in this cycle occurs for a displacement of about 5 nm [15].

Before mechanical contact is established (displacement less than 5 nm in Fig. 1), an attractive long-range force that depends inversely on the displacement is detected. The magnitude of this long-range force is too large to be attributed to van der Waals interactions [16]. Attractive forces before contact, of similar magnitude and dependence, have been observed in force microscopy and explained in terms of patch charges on the surface of the interacting bodies [17]. After contact is established, the force and current curves become hysteretic. The shape of the load-cycle in Fig. 1, and the fact that forces are attractive for the whole cycle show that the long-range interaction is still effective after contact has been established, and suggest its independence of the contact. In order to obtain the force acting on the contact (*mechanical force*), which is responsible for its deformation, it is necessary to subtract the long-range attractive force from the total measured force. We estimate this attractive force by making a smooth interpolation between the tensile and compressive branches of the load-cycle and requiring that the average apparent pressure (ratio of mechanical force to contact area) for a given contact area be of the same magnitude for compressive and tensile forces [18]. In the case of Fig. 1, the resulting curve (thin line) is a smooth extrapolating of the portion of the force curve before contact. This procedure yields consistent results for all the experimental load-cycles (we have analyzed almost 500 experimental cycles). In particular, we find that the average apparent pressure is of the same magnitude for all cycles (for contact radii smaller than 7 nm) and does not depend on contact radius.

In Fig. 3, we show the mechanical force and current variations during the elongation of a neck whose initial radius was 3.1 nm [19]. As the neck is elongated at a constant rate the current decreases stepwise, while the force decreases with an oscillatory sawtoothlike behavior: abrupt relaxations of the force correlate to abrupt decreases of the current. These events occur at 0.1–0.2 nm intervals in the displacement. In between the relaxations the force varies linearly while the current remains almost constant. The contraction of the neck follows a similar process (see Fig. 4), with abrupt relaxations of the force correlating to abrupt increases of the current.

These observations are consistent with molecular dynamics calculations, which predict that the neck deforms through a series of structural transformations involving elastic and yielding stages. The magnitude of the force increases monotonically during the elastic stage, decreasing sharply at the structural transformations [2,3]. The

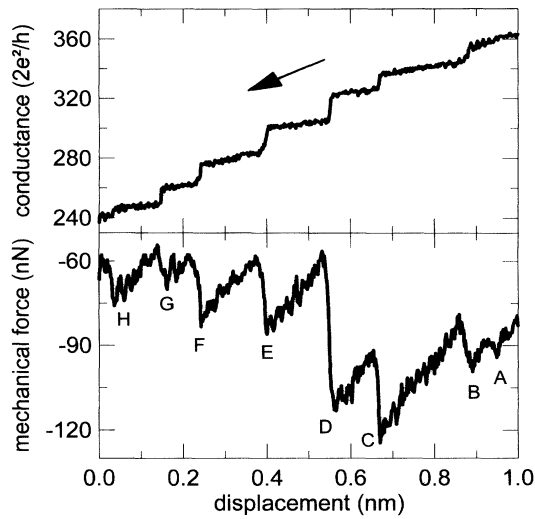


FIG. 3. Deformation under tensile stress: conductance, and mechanical force vs displacement. The conductance is given in units of  $2e^2/h = 77.5 \mu S$ . The minimum pressures (in GPa) before relaxation at the indicated points are  $A = -2.28$ ,  $B = -3.31$ ,  $C = -4.22$ ,  $D = -3.93$ ,  $E = -3.17$ ,  $F = -3.42$ ,  $G = -2.98$ , and  $H = -3.34$ . The neck radius changed from 3.1 to 2.5 nm as the neck was elongated 1 nm.

change in neck section after each structural transformation reflects as an abrupt conductance change [4].

Figure 5 shows a load-cycle of 1 nm amplitude and neck radius varying between 1.5 and 2.1 nm. This cycle starts at the right-hand side of the figure. At the left-hand side where motion changes from tensile to compressive (between points C and D), current and mechanical force

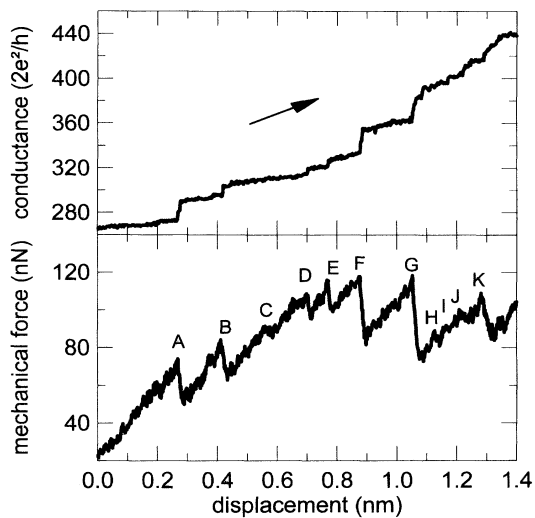


FIG. 4. Deformation under compressive stress: conductance, and mechanical force vs displacement. The maximum apparent pressures (in GPa) before relaxation at the indicated points are  $A = 3.13$ ,  $B = 3.28$ ,  $C = 3.39$ ,  $D = 4.00$ ,  $E = 4.14$ ,  $F = 4.09$ ,  $G = 3.76$ ,  $H = 2.40$ ,  $I = 2.68$ ,  $J = 2.84$ , and  $K = 3.01$ . The neck radius changed from 2.7 to 3.5 nm as the neck was contracted 1.4 nm.

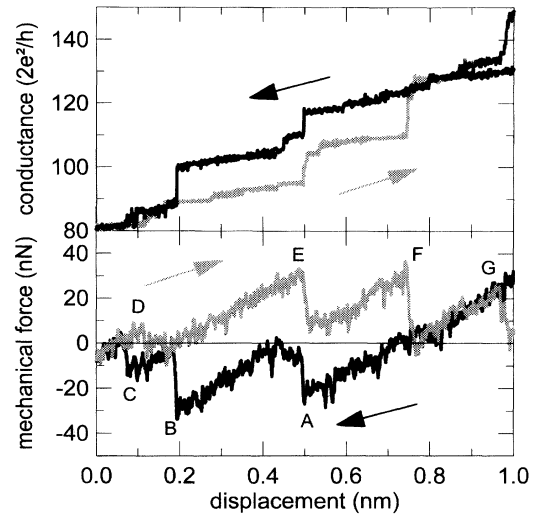


FIG. 5. Small amplitude (1 nm) load-cycle. Grey lines: compressive branch, and black lines: tensile branch. Minimum (tensile) and maximum (compressive) apparent pressures (in GPa) before relaxation at the indicated points are  $A = -2.34$ ,  $B = -3.41$ ,  $C = -1.66$ ,  $D = 1.07$ ,  $E = 3.99$ ,  $F = 3.74$ ,  $G = 1.72$ , and  $H = 2.00$ . During the cycle the neck radius varies between 1.5 and 2.1 nm.

are identical for both branches, illustrating that the motion between structural transformations is reversible. Note also that in this cycle the force relaxes to a value close to zero after the structural transformations.

In order to obtain precise quantitative information on the nanomechanical properties of the connective necks it would be necessary to know their exact shapes. However, taking into account that for a short neck the mechanical properties will not differ much from those of a contact, we can use contact mechanics to obtain approximate quantitative information. The slope of the elastic stages of the mechanical force vs displacement curves defines the effective spring constant of the neck,  $k_{eff} = \text{mechanical force}/\text{displacement}$ . The effective spring constant of a contact is given by [20]

$$k_{eff} = B \frac{aE}{(1 - \nu^2)}, \quad (1)$$

where  $a$  is the radius of the contact,  $E$  is Young's modulus,  $\nu$  is Poisson's ratio (0.42 for Au), and  $B$  is a factor that depends on the exact pressure distribution, i.e., on the geometry of the contact. Realistic limiting values of this factor are  $B = 1$ , corresponding to uniform displacement of the contact area, in which case the pressure is minimum at the center of the contact and diverges on the perimeter, and  $B = 2/3$ , corresponding to Hertzian pressure distribution, in which case the pressure is maximum at the center of the contact and zero on the perimeter. The experimental data show that the effective spring constant depends linearly on the radius  $a$ , and that for a given radius this effective spring constant is of the same magnitude for tensile and compressive

stresses as clearly illustrated in the load-cycle of Fig. 5. For the curves in Figs. 3 and 4,  $k_{\text{eff}} = 240 \text{ N/m}$  and  $a \approx 3 \text{ nm}$ , while for those in Fig. 5,  $k_{\text{eff}} = 138 \text{ N/m}$  and  $a \approx 1.7 \text{ nm}$ , yielding in both cases  $BE \approx 66 \text{ GPa}$ , which is consistent with the macroscopic value of the Young's modulus  $E$  [21] and with  $B$  in the above-mentioned range.

The mechanical strength of the connective neck can be estimated taking into account that for a contact the yield strength  $\sigma_y$  is of the order of the maximum apparent pressure [20]. We can determine the magnitude of the maximum apparent pressure dividing the maximum force before the structural transformations into the area. For the curves in Figs. 3–5 the apparent pressure ranges from 1.7 to 4.2 GPa. The differences in maximum apparent pressure from one point to the other are likely to be related to the degree of disorder of the configuration after a relaxation. For necks of larger radius (from 4 to 8 nm as in Fig. 1) the maximum pressure attains a rather constant value of about 4 GPa. Thus the value of the yield strength is up to 20 times larger than the macroscopic value, and of the same order of magnitude than the theoretical value in the absence of dislocations,  $\sigma_y = 1.5 \text{ GPa}$  for gold [22].

In summary, we have shown that plastic deformation of nanometer-size metal structures proceeds in a sequence of mechanical instabilities as predicted by molecular dynamics simulations. Detailed analysis of the process makes it possible to obtain quantitative information on the elastic and plastic properties of the nanostructures.

We thank J.G. Rodrigo and C. Sirvent for their collaboration in this work. This work has been supported by the CICYT under Contract No. MAT92-0170.

- [1] H. Rohrer, in *Scanning Tunneling Microscopy and Related Methods*, edited by R.J. Behm, N. García, and H. Rohrer (Kluwer, Dordrecht, 1990), p. 1.
- [2] U. Landman, W.D. Luedtke, N.A. Burnham, and R.J. Colton, *Science* **248**, 454 (1990); U. Landman, W.D. Luedtke, and E.M. Ringer, in *Fundamentals of Friction: Macroscopic and Microscopic Processes*, edited by I.L. Singer and H.M. Pollock (Kluwer, Dordrecht, 1992), p. 463.
- [3] R.M. Lynden-Bell, *Science* **263**, 1704 (1994); R.M. Lynden-Bell, *J. Phys. Condens. Matter* **4**, 2127 (1992).
- [4] T.N. Todorov and A.P. Sutton, *Phys. Rev. Lett.* **70**, 2138 (1993); A.P. Sutton, J.B. Pethica, H. Ruffi-Tabar, and J.A. Nieminen, in *Electron Theory in Alloy Design*, edited by D.G. Pettifor and A.H. Cottrell (Institute of Materials, London, 1992), Chap. 7.
- [5] M. Salmeron, A. Folch, G. Neubauer, M. Tomitori, D.F. Ogletree, and W. Kolbe, *Langmuir* **8**, 2832 (1992).
- [6] P. Tangyonyong, R.C. Thomas, J.E. Houston, T.A. Michalske, R.M. Crooks, and A.J. Howard, *Phys. Rev. Lett.* **71**, 3319 (1993); R.C. Thomas, J.E. Houston, T.A. Michalske, and R.M. Crooks, *Science* **259**, 1883 (1993).
- [7] N. Agraït, J.G. Rodrigo, C. Sirvent, and S. Vieira, *Phys. Rev. B* **48**, 8499 (1993).
- [8] N.A. Burnham, D.D. Domínguez, R.L. Mowery, and R.J. Colton, *Phys. Rev. Lett.* **64**, 1931 (1990).
- [9] For the data presented in this work the cantilever was positive with respect to the sample, reversing the polarity did not have any apparent effect on the results. There is no heating of the contact because the bias voltage is low enough and the contact is in the ballistic regime; that is, the contact dimensions are much smaller than the mean free path of the electrons [see A.M. Duif, A.G.M. Jansen, and P. Wyder, *J. Phys. Condens. Matter* **1**, 3157 (1989); J.G. Rodrigo, N. Agraït, C. Sirvent, and S. Vieira, *Phys. Rev. B* **50**, 12788 (1994)].
- [10] N. Agraït, J.G. Rodrigo, G. Rubio, C. Sirvent, and S. Vieira, *Thin Solid Films* **253**, 199 (1994).
- [11] S. Vieira, *IBM J. Res. Dev.* **30**, 553 (1986).
- [12] A.G.M. Jansen, A.P. van Gelder, and P. Wyder, *J. Phys. C* **13**, 6073 (1980).
- [13] J.A. Torres, J.I. Pascual, and J.J. Sáenz, *Phys. Rev. B* **49**, 16581 (1994).
- [14] Further evidence on the cleanliness of the surfaces of the protrusions resulting from breaking the neck is obtained by measuring the apparent tunneling barrier between these opposing protrusions. In our experiment we typically obtain large values of the apparent barrier (about 3.5 eV) indicating the absence of adsorbates: see J.K. Gimzewski and R. Moeller, *Phys. Rev. B* **36**, 1284 (1987).
- [15] N. Agraït, J.G. Rodrigo, and S. Vieira, *Phys. Rev. B* **47**, 12345 (1993); J.M. Krans, C.J. Muller, I.K. Yanson, Th.C.M. Govaert, R. Hesper, and J.M. van Ruitenbeek, *Phys. Rev. B* **48**, 14721 (1993); J.I. Pascual, J. Méndez, J. Gómez-Herrero, A.M. Baró, N. García, and Vu Thien Binh, *Phys. Rev. Lett.* **71**, 1852 (1993).
- [16] J. Israelachvili, *Intermolecular and Surface Forces* (Academic Press, London, 1992).
- [17] N.A. Burnham, R.J. Colton, and H.M. Pollock, *Phys. Rev. Lett.* **69**, 144 (1992).
- [18] This is the observed behavior for macroscopic samples: mechanical properties are the same for compressive and tensile loads. In the microscopic scale molecular dynamics simulations show similar results [2]. Depending on the exact details of the averaging process the obtained attractive force (and consequently the mechanical force) varies by less than 20%.
- [19] For this and all the following figures we have plotted the displacements of the tip with respect to a fixed reference because the movement of the cantilever in these small cycles is about 10% of the amplitude of the cycle.
- [20] K.L. Johnson, *Contact Mechanics* (Cambridge University Press, Cambridge, 1985).
- [21] The Young's modulus depends on the crystalline direction. For Au at 0 K it ranges from 46.5 to 126 GPa; see C. Kittel, *Introduction to Solid States Physics* (Wiley, New York, 1971), 4th ed.
- [22] This value should be regarded only as an order of magnitude estimate; see A. Kelly and N.H. Macmillan, *Strong Solids* (Clarendon, Oxford, 1986); N.H. Macmillan, in *Ideal Strength of Solids*, edited by R.M. Latanision and J.R. Pickens (Plenum, New York, 1981). A similar value for the shear yield stress of Au was obtained in [6]. In a previous experiment on Pb [10], the measured value of the shear yield stress was also of the same order of magnitude as the theoretical value but much larger than the bulk one [10].

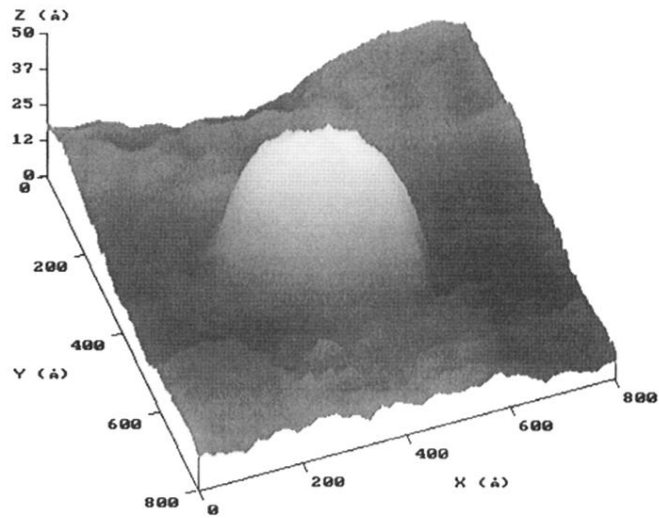


FIG. 2. Protrusion on the substrate after breaking of the connective neck. A series of load-cycles of an amplitude, similar to that of the load-cycle in Fig. 1, were performed on this spot. Bias voltage was 100 mV (tip negative), and the current was 1 nA.